

Electrodynamic interaction between tumor treating fields and microtubule electrophysiological activities

Cite as: APL Bioeng. 8, 026118 (2024); doi: 10.1063/5.0197900

Submitted: 15 January 2024 · Accepted: 1 May 2024 ·

Published Online: 3 June 2024



View Online



Export Citation



CrossMark

Xing Li,¹  Kaida Liu,¹  Haohan Fang,¹ Zirong Liu,¹  Yuchen Tang,¹ and Ping Dai^{2,a)} 

AFFILIATIONS

¹College of Automation Engineering, Nanjing University of Aeronautics and Astronautics, Nan Jing 210016, Jiang Su, China

²Department of Radiotherapy, Shanghai Fourth People's Hospital, School of Medicine, Tongji University, Shanghai 200434, China

Note: This paper is part of the special issue on Physical Sciences Approaches to Cancer Research.

^{a)}Author to whom correspondence should be addressed: daiping@tongji.edu.cn

ABSTRACT

Tumor treating fields (TTFields) are a type of sinusoidal alternating current electric field that has proven effective in inhibiting the reproduction of dividing tumor cells. Despite their recognized impact, the precise biophysical mechanisms underlying the unique effects of TTFields remain unknown. Many of the previous studies predominantly attribute the inhibitory effects of TTFields to mitotic disruption, with intracellular microtubules identified as crucial targets. However, this conceptual framework lacks substantiation at the mesoscopic level. This study addresses the existing gap by constructing force models for tubulin and other key subcellular structures involved in microtubule electrophysiological activities under TTFields exposure. The primary objective is to explore whether the electric force or torque exerted by TTFields significantly influences the normal structure and activities of microtubules. Initially, we examine the potential effect on the dynamic stability of microtubule structures by calculating the electric field torque on the tubulin dimer orientation. Furthermore, given the importance of electrostatics in microtubule-associated activities, such as chromosome segregation and substance transport of kinesin during mitosis, we investigate the interaction between TTFields and these electrostatic processes. Our data show that the electrodynamic effects of TTFields are most likely too weak to disrupt normal microtubule electrophysiological activities significantly. Consequently, we posit that the observed cytoskeleton destruction in mitosis is more likely attributable to non-mechanical mechanisms.

© 2024 Author(s). All article content, except where otherwise noted, is licensed under a Creative Commons Attribution-NonCommercial 4.0 International (CC BY-NC) license (<https://creativecommons.org/licenses/by-nc/4.0/>). <https://doi.org/10.1063/5.0197900>

I. INTRODUCTION

In the early 2000s, the discovery of specific sinusoidal electric fields characterized by low intensity (1–3 V/cm) and intermediate frequency (100–300 kHz) marked a significant advancement in cancer therapy. These electric fields, known as tumor treating fields (TTFields), exhibited a remarkable inhibitory effect on the growth of tumor cells.¹ Notably, TTFields have gained FDA (the Food and Drug Administration) approval as a novel therapy method for glioblastoma (GBM)² and malignant pleural mesothelioma (MPM).³ Despite this regulatory endorsement and the clinical success observed in specific malignancies, the precise mechanisms underlying the therapeutic actions of TTFields remain elusive.

TTFields triggering the mitotic disruption of cancer cells, leading to subsequent cell death, is widely posited as the most likely underlying mechanism. This viewpoint seems to be supported by the following

basic logic: during mitosis, the polymerization and depolymerization of microtubules (MTs) are more active,⁴ suggesting susceptibility to the electric force torque exerted by TTFields on electropolar tubulin dimers. Consequently, this torque aligns them parallel to the external electric field direction, resulting in cytoskeleton destabilization. Ultimately, this cascade effect leads to the disruption of all physiological activities reliant on MTs, culminating in mitotic failure.⁵ Experimental findings, particularly anomalous cytoskeleton fluorescence images observed during TTFields treatment across diverse cancer cell lines,^{6,7} can serve as evidence of TTFields damaging MTs. However, the means by which this occurs, whether through mechanical or non-mechanical mechanisms, remains not fully understood yet. Notably, these experimental phenomena do not constitute direct evidence of MTs being destroyed by the electric field force and torque, as the intricacies of MT polymerization involve not only electric field

forces between dimers but also multifaceted biochemical factors, such as pH values⁸ and ion concentrations⁹ within the chemical microenvironment.

As potential therapeutic targets of TTFields, MTs assume a pivotal role in maintaining normal cell structure and function, including cell migration, mitotic progression, and intracellular transport.¹⁰ Structurally, MTs are hollow cylindrical protein tubes with external diameters of approximately 25 nm and lengths extending to tens of micrometers.¹¹ The basic unit of MTs is a special protein dimer polymerized by α and β tubulin, also referred to as α and β monomers.¹² Remarkably, electron crystallography measurements reveal that the protein structures of α and β monomers exhibit nearly identical spherical configurations, each possessing a molecular weight of about 55 kDa.¹³

Electrical activities play a significant role in many MT functions. For instance, in intracellular substance transport, MTs act as bridges for kinesins to walk on, facilitating their movement. Electrostatic attractions between kinesins and MTs ensure the directed motion of kinesins along the MTs without detachment.¹² Furthermore, the orchestrated movement of chromosomes during mitosis hinges upon the electric attraction between microtubule ends and the centrosome.¹⁴ These electrodynamic intricacies underscore the indispensable role of electrical phenomena in modulating key cellular processes mediated by MTs.

To explore the electrical activities of MTs, previous studies conducted meticulous examinations of the electric properties of tubulins through molecular dynamics (MD) simulations. The findings revealed that tubulin is highly negatively charged at physiological pH and possesses an electric dipolar nature, with an overall dipole moment of approximately 1700 D, excluding the C-terminus of the dimer due to its symmetrical structure offsetting the contribution to the electric dipole moment.^{15,16} Moreover, this exploration extended to electromechanical vibrations of MTs,^{17,18} interactions between external electric fields and tubulins,^{11,19,20} as well as interactions between MTs and essential cellular components such as motor proteins and kinetochores.^{4,12,21,22} These investigations revealed that the electrostatic characteristics of MTs emerge as pivotal determinants governing the aforementioned activities.

Although the hypothesis that TTFields may disrupt the orientation of tubulin dimers through electric field torque is widely acknowledged in the context of tumor treating fields (TTFields) mechanisms, it currently lacks comprehensive theoretical substantiation, even some studies have yielded qualified results in regard to this hypothesis.^{23–25}

This study is designed to build upon the previous knowledge gained in Ref. 23 by conducting a more comprehensive examination of the interaction between TTFields and MTs, as well as its potential impact on MTs' electrophysiological activities. We address this issue by constructing comprehensive analytical and numerical models to characterize and calculate the electric force and torque generated by TTFields on tubulin, chromosomes, and kinesin. The theoretical study indicates that TTFields manifest as weak electric fields incapable of generating forces and torques of sufficient magnitude to disrupt normal electrophysiological activities that rely on MTs. This suggests that TTFields might influence MT structures and functions through other biochemical or electric mechanisms, rather than through direct mechanical effects. These findings support the need for a different perspective when seeking to understand the intricacies of TTFields'

impact on MTs compared to existing hypotheses, such as TTFields activate ion channels²⁶ or increase the cell membrane permeability,²⁷ resulting in microenvironmental disturbance in the cytoplasm.

II. RESULTS

This section presents the theoretical calculations and corresponding simulation outcomes derived from typical model data. A more extensive comparative analysis and discussion will be undertaken in Sec. III.

A. Impact of TTFields torque on dimer orientation

A typical TTField comprises a sinusoidal alternating electric field with a peak value of 2 V/cm and a frequency of 200 kHz.¹ While a previous study has indicated a slight decrease in the external TTFields penetrating into the intracellular cytoplasm due to voltage drop on the cell membrane,²³ in this study, we assume an amplitude of E at 2 V/cm in the torque calculations [Eq. (2)] to establish an upper limit for potential effects.

The initial orientations of microtubule dimers in the cytoplasm are random due to Brownian motion. To encompass all possible scenarios, we calculated the torque spectrum that contribute to the rotation of a single dimer within one TTFields period, as depicted in Fig. 1. It is important to emphasize that when the initial orientation $\theta = 0$, in accordance with the definition of θ outlined in Fig. 6, the long axis of the dimer is not vertical; rather, the electric dipole moment is vertical.

Figure 1 presents a torque distribution spectrum observed when the dimers are exposed to TTFields. It becomes evident that for dimers with various initial orientations, the range of TTFields torque spans approximately from 0 to 1.48×10^{-24} Nm (without considering torque directions). The torque reaches its maximum when the electric field direction is perpendicular to the dimer's dipole moment and sinusoidal TTFields reach their peak value ($t = T/4$). A rough estimation reveals that the maximum torque is significantly less than the thermal energy

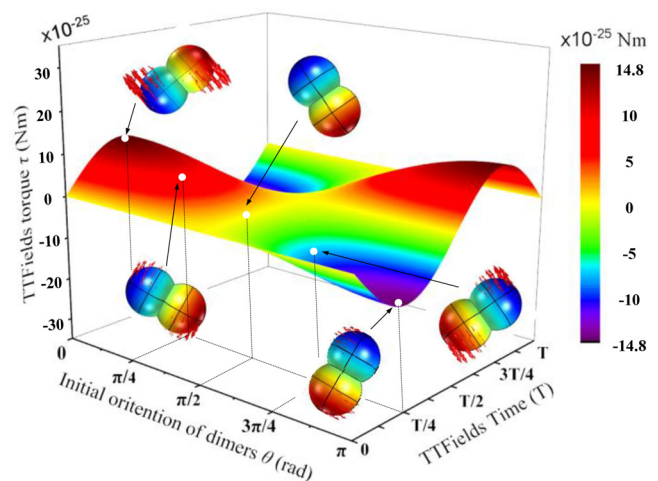


FIG. 1. Torques contribute to the rotation of dimers caused by TTFields, and clockwise is defined as the positive direction. Typical values (TTFields reaches the amplitude at $T/4$; dimer initial orientations: $0, \pi/4, \pi/2, 3\pi/4, \pi$) are marked with white dots in the figure, and corresponding torque simulation results are also presented.

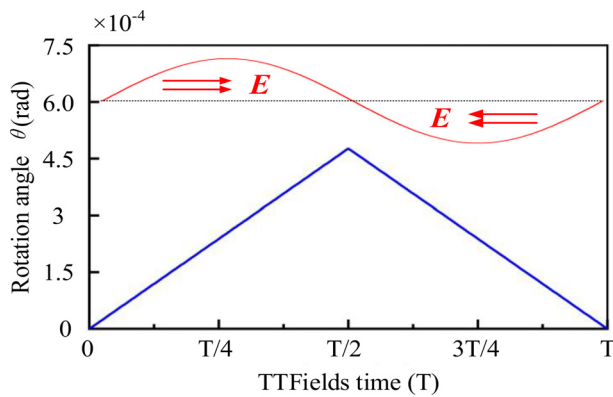


FIG. 2. Rotation angle of the dimer within one TTFIELDS period; the red line shows the TTFIELDS wave.

$k_B T$, which is approximately 4.3×10^{-21} J (where k_B represents Boltzmann’s constant, approximately 1.38×10^{-23} J/K, and T represents the normal body temperature, approximately 310 K). This observation suggests that the torque is unlikely to exert a substantial influence on dimer orientations. Given the pivotal role of dimer orientations in the microtubule (MT) polymerization process, it is reasonable to suggest that the relatively subtle torque exerted by TTFIELDS may not significantly disrupt the dynamic stability of MT structure, for instance, its normal extension and retraction rely on the orchestrated disassembly and assembly of dimers.

Moreover, to intuitively assess the impact of TTFIELDS torque on dimer orientation, we selected a dimer with an initial orientation of 0 as an illustrative example. We solved Eq. (4) to calculate its rotation angle within a single TTFIELDS period. The viscosity coefficient of the cytoplasm was set at 2 mPa s,^{28,29} and all other relevant parameters have been detailed in Sec. IV. The results are presented in Fig. 2.

Figure 2 illustrates that during the first half of the TTFIELDS period, the rotation angle of the dimer reaches a maximum of approximately 4.9×10^{-4} rad (approximately 101 arc sec) and then gradually decreases during the second half of the period. This behavior is a result of the torque’s direction remaining consistent in the first half, leading to an accumulated rotational effect. Conversely, in the second half of the period, the torque’s direction reverses, causing the dimer to rotate in the opposite direction.

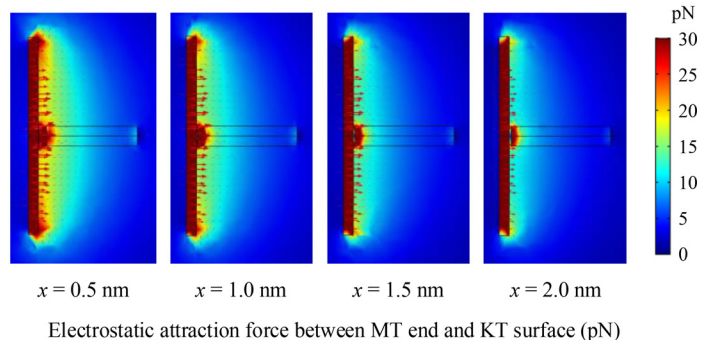
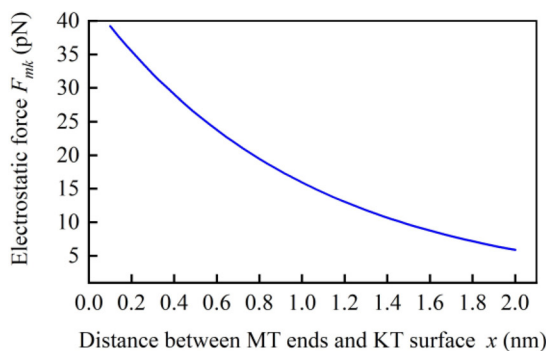


FIG. 3. The electrostatic attractive force between MT ends and KT surface; left panel: theoretical calculation results and right panel: simulation results.

It is important to emphasize that while this calculation is based on a specific case, the result indicates that TTFIELDS torque can induce a rotation angle on the order of 10^{-4} rad in the dimer, which has an insignificant impact on their random orientations. This outcome can be attributed to the viscosity of the cytoplasm and the alternating direction change of the TTFIELDS.

B. Impact of TTFIELDS force on chromosome traction

We solved Eqs. (5)–(8) with the finite element solution to Eqs. (13) and (15) to assess the TTFIELDS force on the MT end and KT plate. The results were then compared with the inherent electrostatic attraction force to evaluate the effect of TTFIELDS on chromosome movement. In Eq. (7), given the absence of direct experimental data on the surface charge density σ of the KT plate, we assigned a reasonable value of 25 mC/m², falling within the typical range of biological protein surfaces.^{30,31} Additionally, we assigned typical values of 60 for the relative permittivity and 1 nm for the Debye length for the cytoplasm.³² The surface area of the KT was approximately estimated as $0.2 \mu\text{m}^2$ (diameter 500 nm), aligning with the earlier order of magnitude estimation of $\sim 10^2$ nm. We calculated the attractive force between one MT end and the KT plate. The results of the calculations are displayed in Fig. 3.

The data extracted from Fig. 3 indicates that the attractive force diminishes as the distance increases. The overall values are within the range of piconewtons to tens of piconewtons, which closely aligns with experimental results.³³ The TTFIELDS forces on the MT ends (denoted as F_{Em}) and similarly on the KT plate (denoted as F_{Ek}) are calculated to be $F_{Em} = 3.6 \times 10^{-4} \sin(4\pi \times 10^5 t)$ pN and similarly $F_{Ek} = 1.0 \sin(4\pi \times 10^5 t)$ pN. These calculated values show that the amplitudes of F_{Em} and F_{Ek} are significantly smaller than the normal attractive force. As a result, it is unlikely that TTFIELDS forces would disrupt normal chromosome movements.

C. Impact of TTFIELDS force on kinesin-MT bonding

An important function of MT’s in intracellular substance transportation is to serve as a substrate for kinesins advancing on them. Although the mechanisms of kinesin stepping along the MT surface are intricate and not fully elucidated, electrostatic interactions are believed to play a pivotal role in this process.¹² Figure 8 is a representation of the forces between the kinesin and MT, as well as the torque rotation effect on kinesin dipole moment, when tumor cells are exposed to TTFIELDS. We calculated the attractive forces at various

bonding strengths by setting different distances from the kinesin head to the surface of the MT. The charge of the kinesin motor domain and MT surface charge density are set as $+5e$ and -37 mC/m^2 , respectively, in accordance with prior studies.^{12,30} Likewise, the Debye length of the cytoplasm is set as 1 nm. The results of the calculations and the results of the simulation of electrostatic attraction are presented in Fig. 4. Moreover, to investigate whether the TTFields torque acting on the kinesin dipole moment and the electric tension force exerted on the C-terminus of β monomer significantly influence the attachment of kinesin to the MT, we calculated the maximum TTFields force and torque. Subsequently, we conducted a comparative analysis with recent research findings.²¹

The data in Fig. 4 indicate that the attractive force is consistently within the range of tens of piconewtons. Considering the known step distance of kinesin, which is approximately 4 nm,³⁴ we can estimate that the motor domain area of kinesin on the MT surface is likely less than $1.26 \times 10^{-13} \text{ m}^2$ (assuming the domain is circular with a diameter of 4 nm). Consequently, the maximum pulling forces generated by TTFields on the kinesin motor domain and MT surface are approximately 1.6×10^{-4} and 1.0×10^{-4} pN, respectively. Therefore, the results indicate that although the opposite TTFields force has a tearing effect that could potentially disrupt the binding between MT and kinesin, it is too weak (approximately 10^{-4} pN vs tens of piconewtons) to exert an effective impact. Additionally, the kinesin exhibits an overall dipole moment of approximately 1200 D, with potential fluctuations ranging from 100 to 400 D when subjected to electric fields of 100 MV/m.²¹ Given that the magnitude of TTFields is significantly lower than 100 MV/m, we set the kinesin dipole moment value at 1200 D and calculated the torque using Eq. (13) to be approximately 8.0×10^{-25} Nm. Similarly, this torque is substantially smaller than the normal physiological thermal energy $k_B T$, that is $\sim 4.3 \times 10^{-21}$ J. The C-terminus of β monomer carries a negative charge of approximately $-19e$,²¹ and the tension force induced by TTFields is estimated to be about 6.1×10^{-4} pN; however, this value is considerably less than the normal inherent electrostatic force, which typically ranges in the tens of piconewtons. Based on the above-mentioned comprehensive analysis results, we believe that TTFields are less likely to detach the kinesin from the MT through electric force and torque.

III. DISCUSSIONS AND CONCLUSIONS

Our investigation shows that the electrodynamic effects induced by TTFields' force and torque on the microtubule structure, as well as

its associated electrophysiological functions, such as chromosome driving and kinesin stepping, are exceptionally weak. In our calculations, we have confirmed that the intrinsic electrostatic attractive forces between microtubules and kinetochores, as well as kinesins, typically range from piconewtons to tens of piconewtons. These values align with typical forces observed in numerous subcellular structure interactions reported in prior studies. For example, optical tweezers experiments demonstrated that each protofilament's bending stiffness could generate a force of approximately 2.3 pN, with a total force of approximately 30 pN for the 13 protofilaments in one microtubule.²²

Mechanical analysis indicates that as kinesin walks on the microtubule surface, it can carry a load of up to 6–8 pN.³⁵ In mechanical separation experiments of DNA, it was found that the force required to pull apart the double helix of a DNA molecule is ~ 100 pN.³⁶ However, the electric forces generated by TTFields on MT, KT plate, and kinesin heads are notably smaller than the intrinsic typical values, indeed, smaller by an order of magnitude. Therefore, based on our calculations, we can reasonably assert that the strength of TTFields is insufficient to exert direct mechanical effects on subcellular structures.

This conclusion gains further support from historical data regarding external electric field strength. For instance, electro-orientation experiments have demonstrated that alternating electric fields required to orient random microtubules must reach approximately 10^5 V/m.³⁷ A previous study suggests that the tubulin–tubulin binding energy is very high, specifically around 20 kcal/mol; therefore, the lowest electric field strength capable of electro-opening the microtubule lattice could be approximately 10 MV/m.¹¹ Recent studies focusing on the application of nanosecond pulsed electric fields to detach kinesin from the MT indicate that significant detachment effects are observed when the electric field intensity reaches tens of millivolt/meter.^{21,38} Furthermore, even in a study where the electric field strength was lower than 100 MV/m, it did not appear to cause any discernible effect on tubulin structure,²⁰ among other instances documented in the literature.

Theoretical calculations and FEM simulations are the primary research methods employed in this work. All our calculations and models are based on typical parameters from previous studies, experimental reports, and other reliable sources. Even if there are slight deviations in these parameters, they are unlikely to result in significant differences in the results. For example, in the literature,^{14,15,20,30,37} the net negative charge of a tubulin monomer ranges from a few to dozens of electron charges. Consequently, the TTFields electric force on MT ends will range from 10^{-4} to 10^{-5} pN, which is still much weaker than

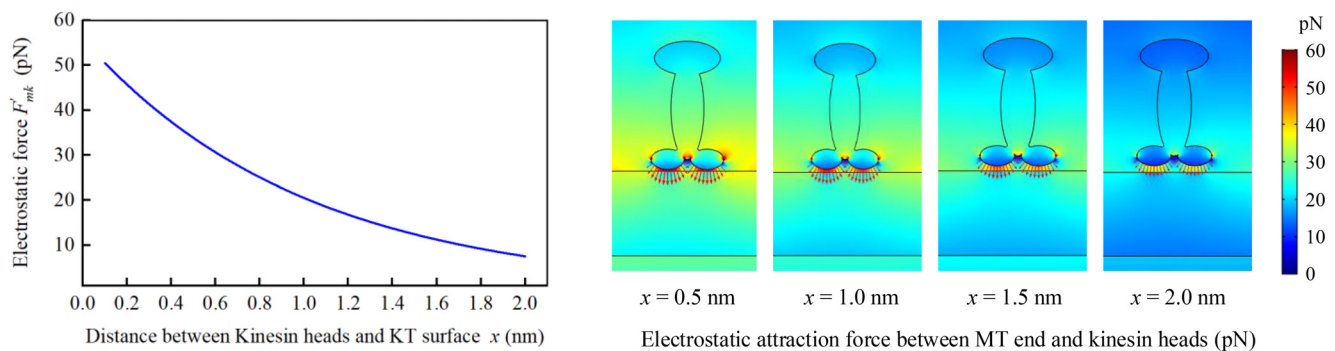


FIG. 4. The electrostatic attractive force between MT surface and kinesin head; left panel: theoretical calculation results and right panel: simulation results.

the attractive force (tens of piconewtons) between MT and KT plate. The dipole moment of a single tubulin dimer varies slightly across different references, particularly showing a slight increase when considering the C-termini.²⁰ Even considering the overall electric dipole moment including the C-termini, the electric field torque is expected to have minimal effect on the rotation of the dimer induced by TTFields torque. Therefore, we have confidence that our theoretical analysis results are reliable.

At the tissue level, TTFields cancer therapy demonstrates minimal side effects, primarily manifesting as mild dermatitis beneath the electrodes. Furthermore, TTFields can selectively inhibit tumor cell proliferation while exerting minimal impact on healthy tissue. Therefore, TTFields therapy can be a very promising modality for tumor treatment. However, the mesoscopic mechanisms of TTFields therapy are still elusive. In contrast to numerous previous studies on the mechanism of TTFields, our findings lead to a different conclusion, suggesting that TTFields are almost unlikely to directly disrupt microtubule structure and its main associated electrophysiological activities through electrodynamic impacts. Nevertheless, we must emphasize that we are not refuting the fact that TTFields inhibit cancer cell proliferation by inducing mitosis destruction. However, our research proposes that the underlying mechanisms of how TTFields cause mitosis destruction, especially microtubule structure damage and chromosome segregation abnormalities, may be attributed to non-mechanical effects. For instance, the concentrations of Ca^{2+} and Mg^{2+} in the cytoplasm are notable factors that affect MT tubulin polymerization, and corresponding preliminary experiments have indicated significant changes in cytoplasmic calcium ion concentration when tumor cells are exposed to TTFields.²⁶ In summary, the mechanisms of TTFields remain elusive, and indirect mechanical actions like biochemical effects may play critical roles in inhibiting cancer cell growth by disrupting mitosis. We hope this work stimulates further research interest in understanding the molecular-level mechanisms of TTFields.

IV. METHODS

A. Models of microtubule and tubulin dimer

MTs are approximately hollow cylinders assembled from $\alpha\beta$ tubulin dimers, and the structure and dimensions of a single MT are depicted in Fig. 5(a). Typically, MTs are composed of 13 protofilaments (PFs), with each PF consisting of tubulin dimers arranged in a head-to-tail formation. In 1998, electron crystallography confirmed

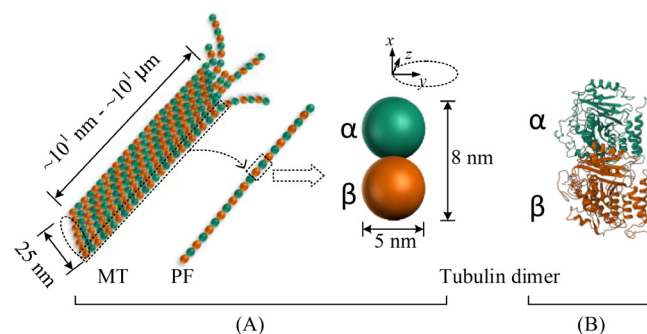


FIG. 5. Physical structures and models of MT, PF, and tubulin dimer: (a) cylinder-like structure of the MT and spherical dimer and (b) the protein structure of tubulin dimer.

the protein structure of $\alpha\beta$ tubulin for the first time, as illustrated in Fig. 5(b) (downloaded from the RCSB Protein Data Bank, PDB),¹³ at a resolution of 3.7 Å. The geometrical shape of α and β monomers is approximately spherical, with a diameter of approximately 5 nm and an axial length of about 8 nm.^{22,39} Therefore, the tubulin dimer can be simply modeled as two intersecting spheres.

Regarding their electric properties, MTs generally exhibit a negative charge in the human body's normal physiological environments (pH \sim 7.2), primarily due to the residual carboxyl terminus.¹⁵ Because the charge distribution is extremely uneven, tubulin proteins display electropolar characteristics. Molecular simulations were conducted to calculate the electric dipole moment of the tubulin dimer,¹⁵ and the results are summarized in Table I. It is important to note that data in Table I did not include the contribution of the C-termini. While this may have a slight effect on the electric dipole moment along the long axis (x-component) due to the symmetrical nature of the C-termini negative charges, it significantly affects the y-dipole moment. Incorporating the C-termini charge results in an approximately 30% increase in the overall dipole moment of a single dimer to 2166 D.²⁰ In order to capture the maximum rotation torque caused by TTFields electric force, we incorporate the overall dipole moment into our calculations when determining the TTFields torque. The coordinate system used to quantify the dimer dipole moment is defined as follows: x represents the MT axial direction from α to β monomer, y is the radial direction toward the MT center axis, and z represents the tangent direction of the MT cylinder surface.

B. Model of TTFields torque effect on tubulin dimer orientation

As shown in Table I, the tubulin dimer possesses a distinct electric dipole moment. When the electric field direction deviates from a parallel alignment with the dipole moment of the dimer, the resulting electric field force induces a torque on the dimer, potentially causing it to rotate from its initial orientation. Considering the viscous nature of the cellular cytoplasm, we take into account the viscous resistance opposing the direction of rotation. Consequently, we formulate a force model for a single dimer, as illustrated in Fig. 6. To simplify the model, we omit the consideration of forces arising from random thermal collisions; we will provide an estimation comparing electric torque and thermal energy in Sec. II.

Assume the rotation center is the binding point of α and β tubulin, the law of rigid body rotation yields

$$M_E + M_f = J\alpha, \quad (1)$$

where M_E is the TTFields torque, M_f is the viscous resistance torque, and J and α are the moment of inertia and angular acceleration of the

TABLE I. Dipole moment of tubulin dimer.

Dipole moment of $\alpha\beta$ dimer	Values (D)
x component	337
y component	-1669
z component	198
Overall	1714

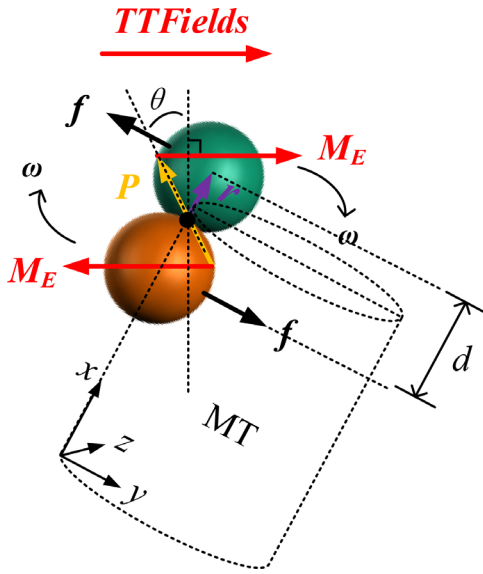


FIG. 6. The force model of dimer rotation under TTFields torque (red arrows) and viscous resistance (black arrows); the yellow arrow presents the overall dipole moment of single dimer.

rotation, respectively. The torques in Eq. (1) can be computed as follows:

$$\begin{cases} \mathbf{M}_E = \mathbf{p} \times \mathbf{E}, \\ \mathbf{M}_f = 2\mathbf{r} \times \mathbf{f}, \\ \mathbf{f} = -6\pi r_0 \eta \mathbf{v}, \end{cases} \quad (2)$$

where \mathbf{p} is the overall dipole moment vector and \mathbf{E} is the TTFields intensity. In Eq. (3), \mathbf{r} is the vector directed from the center of rotation to the centroid of the tubulin monomer, the resistance force \mathbf{f} is achieved by Stocks equation,²⁸ r_0 is the radius of the monomer that is approximately equal to r , η is the cytoplasmic viscosity coefficient, and \mathbf{v} is the linear velocity of dimer rotation and $\mathbf{v} = \omega \mathbf{r}$.

Combining the geometrical conditions shown in Fig. 6, the rotation angle of dimer can be determined by solving the following equation:

$$\frac{d^2\theta}{dt^2} = -\frac{6\pi\eta r}{m} \frac{d\theta}{dt} + \frac{2pE}{md^2} \cos\theta, \quad (4)$$

where θ is the dimer rotation angle from vertical position.

C. Model of TTFields force effect on chromosome movement

During mitosis, the movement of chromosomes is primarily orchestrated by the traction exerted by microtubules acting on the chromosome arms or kinetochore (KT).⁴⁰ This movement is further facilitated by the driving force resulting from electrostatic attraction.¹⁴ With a sufficiently robust attractive force, chromosomes undergo directed motion toward both poles and the equator of the dividing cell, controlled by MTs disassembly (shortening) and assembly (lengthening).

As explained in earlier studies, the attractive force can be attributed to the Coulomb force arising from the positively charged KT surface and negatively charged MT plus ends.¹⁴ Consequently, when the cell is exposed to TTFields, electric forces acting on the KT surface and MT ends become opposing, potentially disrupting the original attractive interactions. In considering the most extreme scenario, the pulling force reaches its maximum when the electric field is parallel to the microtubule axis. We exclusively examine this case to assess the strongest impact of TTFields force on chromosome movement. The corresponding force model can be illustrated as shown in Fig. 7.

The kinetochore is a disk-shaped protein complex whose size can fluctuate based on the cell cycle phase, typically ranging from hundreds of nanometers ($\sim 10^2$ nm) to micrometers ($\sim \mu\text{m}$).⁴¹ In comparison with the size of the MT end (diameter ~ 25 nm), the KT can be approximated as a substantially large, flat plate. Assuming the KT has a uniform charge density σ on its surface, the electric field intensity generated by the KT in the electrolyte cytoplasm is given by

$$E_k = \frac{\sigma}{2\epsilon} e^{-\frac{x}{d}}. \quad (5)$$

Considering that MT ends are consistently perpendicular to the KT surface, it is noteworthy that only the x -component dipole moment significantly contributes to the electrostatic attraction force between KT and MT ends. According to the definition of electric dipole moment, the α and β tubulin are assumed to bear an equal quantity of heterogeneous charges to generate the x -dipole moment. While this assumption might not precisely mirror the nuanced biophysical reality, it ensures mathematical consistency in maintaining the physical effects, that is,

$$p_x = q \cdot (2r) = qd. \quad (6)$$

Hence, the electrostatic attraction force between KT and one MT end (typically includes 13 PFs) can be calculated as

$$F_{mk} = \frac{13\sigma p_x}{2\epsilon d} e^{-\frac{x}{d}}. \quad (7)$$

When the cell is subjected to TTFields, electric forces F_{Ek} and F_{Em} acting on the KT and MT end are

$$\begin{cases} F_{Ek} = \sigma SE, \\ F_{Em} = \frac{13p_x E}{d}, \end{cases} \quad (8)$$

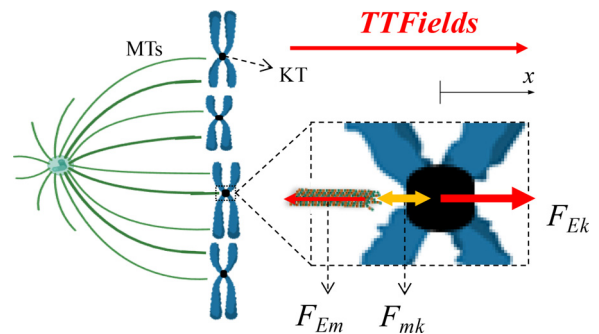


FIG. 7. The force model of TTFields repulsion effect (red arrows) on the inherent electrostatic attraction (yellow arrow) between MT end and KT.

where in Eqs. (5)–(8), ϵ and D are the permittivity and the Debye length of cytoplasm,⁴² respectively; σ and S are the surface charge density and area of KT plate, respectively; x is the distance to the KT surface; p_x is the x -direction dipole moment of the single dimer; d is the distance between monomer centroids; and E is the TTFields intensity.

By comparing the magnitude of TTFields electric force and the inherent attractive force, we can assess the potential electrodynamic impact of TTFields on the chromosome motion.

D. Model of TTFields force effect on kinesin-MT bonding

Motor proteins constitute a vital class of molecular machinery within living cells. Kinesins belong to a superfamily of these proteins. Kinesins facilitate the unidirectional transport of substances toward the microtubule (MT) plus end through a head-over-head walking mechanism along the MT surface. Previous studies^{12,43} have indicated that electrostatic interactions play a pivotal role in assisting kinesin in maintaining a secure binding configuration on the MT, preventing derailment. Importantly, to generate electrostatic attraction, since the MT surface exhibits a negative potential, the motor domain of kinesin is predominantly positively charged, consistent with the electric field computation results surrounding the kinesin,¹² and the net charge of the kinesin is negative, roughly $-5e$.²¹ To determine whether the TTFields electric force can disrupt the binding state, we examine the upper limit where the electric field is perpendicular to the MT surface. In this configuration, TTFields will generate the maximum electric force to repel kinesin from the MT surface. The corresponding force model is depicted in Fig. 8(a). In addition to the electrostatic attraction between the kinesin motor domain and the microtubule (MT) surface, the collective electric dipole moment of kinesin, along with the negatively charged C-terminus of β monomer, plays a significant role in facilitating the binding of kinesin to the MT.²¹ To further investigate the influence of the electric force and torque generated by TTFields on the C-terminus of β monomer and the kinesin's dipole moment, respectively, we conducted

an analysis to determine the maximum impact on the orientation of kinesin. This was achieved by configuring the direction of TTFields to be perpendicular to the dipole moment, as depicted in Fig. 8(b) within our physical model.

To calculate the electric attractive force between kinesin head and MT surface, the MT can be simplified as a uniformly charged cylindrical surface,³⁰ and the surface electric field intensity can be obtained from Gaussian law as

$$E_m = \frac{\sigma_m}{\epsilon} e^{-\frac{x}{D}}. \tag{9}$$

Similarly, the electrostatic attraction force between kinesin head and MT surface can be calculated as

$$F'_{mk} = \frac{\sigma_m q_k}{\epsilon} e^{-\frac{x}{D}}. \tag{10}$$

The electric forces of TTFields on the kinesin motor domain and MT can be expressed, respectively, as

$$\begin{cases} F'_{Ek} = q_k E, \\ F'_{Em} = \sigma_m S_k E, \end{cases} \tag{11}$$

where σ_m is the surface charge density of MT, x is the distance to the MT surface, ϵ and D are the cytoplasm permittivity and the Debye length, respectively, q_k and S_k are the charge quantity and area of kinesin motor domain (head), respectively, and E is the TTFields intensity.

The electric force on C-terminus of β monomer and torque on kinesin generated by TTFields can be calculated as

$$\begin{cases} F_{\beta C} = q_{\beta C} E, \\ \tau_K = p_K E, \end{cases} \tag{12}$$

where $q_{\beta C}$ and p_K are the charge of the C-terminus of β monomer and overall dipole moment of the kinesin, respectively, and E is the TTFields intensity.

By comparing the forces calculated using Eqs. (9)–(12), we can determine whether TTFields will disrupt the typical binding state of kinesin.

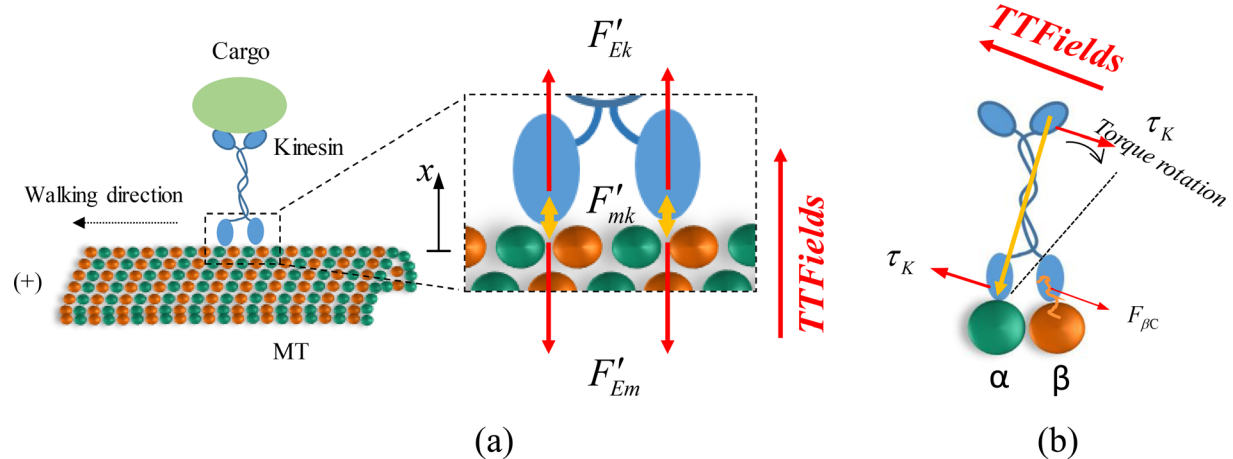


FIG. 8. The physical models of the impact of TTFields on kinesin bonding to the MT. (a) TTFields electric force (red arrows) counteracts the electrostatic attraction (yellow arrows) between the MT surface and kinesin head. (b) TTFields electric force (red thin arrow) on the C-terminus of β monomer and rotation effect on kinesin dipole moment (yellow arrows) caused by TTFields torque (red bold arrows on kinesin).

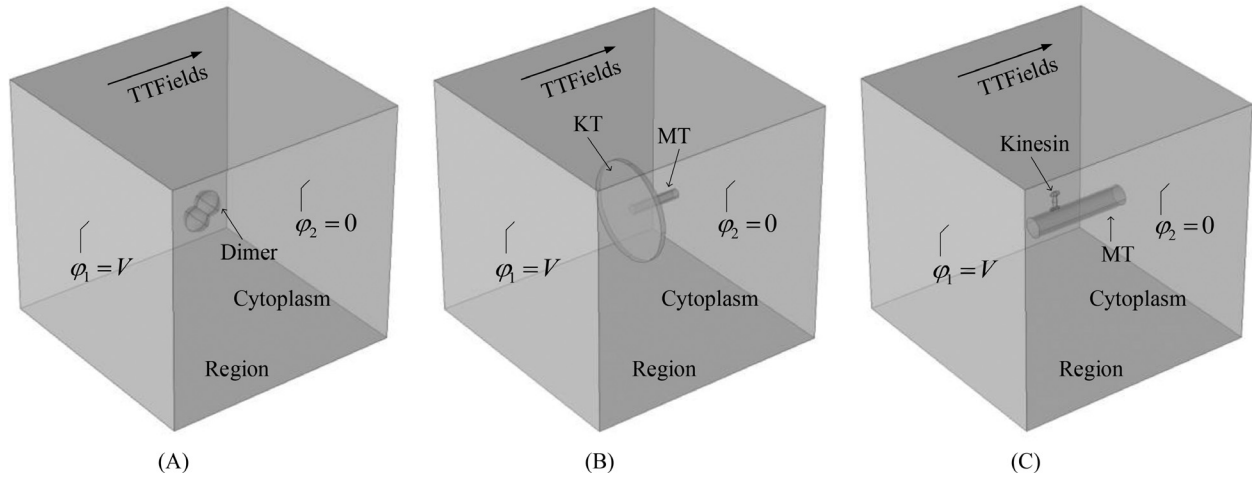


FIG. 9. FEM simulation models: (a) TTFIELDS torque effect on tubulin dimer, (b) electrostatic interaction between MT and KT, and (c) electrostatic interaction between MT and kinesin.

E. Theoretical analysis and simulation verification

We conducted a theoretical analysis to evaluate the electrodynamic effects of TTFIELDS concerning normal microtubule electrophysiological dynamics. Our calculations and comparative analyses utilized typical data from physical models, including geometric and electrical properties.^{12,15,20–23,31,41–43} To enhance the precision of our theoretical calculations compared to previous studies such as,²⁴ we performed finite element method (FEM) simulations using the AC/DC module in COMSOL. Figure 9 and Table II provide details of the corresponding models and their parameters. With the FEM software, we simulated the electric torque on the dimer and the electrostatic forces between KT and MT, as well as between kinesin and MT. These more realistic simulation results reinforce and further validate our calculated results.

In the simulations, the electric field is derived from the Maxwell equation as

$$\nabla \cdot \left(\sigma \mathbf{E} + \epsilon \frac{\partial \mathbf{E}}{\partial t} \right) = 0. \tag{13}$$

The TTFIELDS are generated by a certain boundary voltage excitation,

$$\begin{cases} \varphi_1 = V, \\ \varphi_2 = 0. \end{cases} \tag{14}$$

The relationship between electric field and potential is

$$\mathbf{E} = -\nabla \varphi. \tag{15}$$

The electric forces and torques acting on the subcellular structures are obtained from the solution of Eqs. (2), (8), (11), and (12). In all three simulations, the mesh size consists of approximately 10^5 elements.

TABLE II. Parameters of simulation models.

Parameters		Model A		Model B		Model C		
Electric parameters	Conductivity (S/m)	Cytoplasm	0.5 (Ref. 23)	Cytoplasm	0.5 (Ref. 23)	Cytoplasm	0.5 (Ref. 23)	
		Dimer	0.1 (Ref. 30)	KT	0.1 (Ref. 30)	Kinesin	0.1 (Ref. 30)	
	Relative permittivity	Cytoplasm	60 (Ref. 23)	MT	0.1 (Ref. 30)	MT	0.1 (Ref. 30)	
Dimer		2 (Ref. 43)	Cytoplasm	60 (Ref. 23)	Cytoplasm	60 (Ref. 23)		
Charge or dipole moment	Dimer	2166 D (Ref. 20)	KT	2 (Ref. 43)	Kinesin	2 (Ref. 43)		
			MT	2 (Ref. 43)	MT	2 (Ref. 43)		
			KT	25 mC/m ² (Ref. 35)	Kinesin	+5e (Ref. 12)		
Geometrical parameters (nm)	Region	50 × 50 × 50	MT	−4e (Ref. 15)	MT	−37 mC/m ² (Ref. 30)		
			Dimer	5 × 5 × 8 (Ref. 15)	Region	500 × 500 × 500	Region	500 × 500 × 500
			KT	200 × 200 × 10 (Ref. 41)	KT	20 × 20 × 100 (Ref. 15)	Kinesin	15 × 10 × 30 (Ref. 12)
			MT	20 × 20 × 100 (Ref. 15)	MT	30 × 30 × 200 (Ref. 15)		

ACKNOWLEDGMENTS

This work was supported by Shanghai Fourth People's Hospital, School of Medicine, Tongji University, Talent Introduction and Scientific Research Startup Project No. SYKYQD10101, and China Ministry of Science and Technology Senior Foreign Expert Recruitment Program No. G2023181006L.

AUTHOR DECLARATIONS

Conflict of Interest

The authors have no conflicts to disclose.

Ethics Approval

Ethics approval is not required.

Author Contributions

Xing Li: Conceptualization (equal); Funding acquisition (equal); Investigation (equal); Writing – original draft (equal). **Kaida Liu:** Methodology (equal); Software (equal). **Haohan Fang:** Data curation (equal); Writing – review & editing (equal). **Zirong Liu:** Software (equal). **Yuchen Tang:** Software (equal); Writing – review & editing (equal). **Ping Dai:** Funding acquisition (lead); Methodology (equal).

DATA AVAILABILITY

The data that support the findings of this study are available from the corresponding author upon reasonable request.

REFERENCES

- ¹E. D. Kirson *et al.*, “Disruption of cancer cell replication by alternating electric fields,” *Cancer Res.* **64**(9), 3288–3295 (2004).
- ²J. P. Fisher and D. C. Adamson, “Current FDA-approved therapies for high-grade malignant gliomas,” *Biomedicines* **9**(3), 324 (2021).
- ³T. Kutuk *et al.*, “Feasibility of tumor treating fields with pemetrexed and platinum-based chemotherapy for unresectable malignant pleural mesothelioma: Single-center, real-world data,” *Cancers* **14**(8), 2020 (2022).
- ⁴S. Khwaja *et al.*, “Microtubule associated proteins as targets for anticancer drug development,” *Bioorg. Chem.* **116**, 105320 (2021).
- ⁵S. Yao *et al.*, “Implantable, biodegradable, and wireless triboelectric devices for cancer therapy through disrupting microtubule and actins dynamics,” *Adv. Mater.* **35**(40), 2303962 (2023).
- ⁶A. F. Kessler *et al.*, “Effects of tumor treating fields (TTFields) on glioblastoma cells are augmented by mitotic checkpoint inhibition,” *Cell Death Discovery* **4**, 77 (2018).
- ⁷A. Volodin *et al.*, “Tumor treating fields (TTFields) hinder cancer cell motility through regulation of microtubule and actin dynamics,” *Cancers* **12**(10), 3016 (2020).
- ⁸C. S. Regula and R. D. Berlin, “Microtubule assembly and disassembly at alkaline pH,” *J. Cell Boil.* **89**(1), 45–53 (1981).
- ⁹V. Gal, S. Martin, and P. Bayley, “Fast disassembly of microtubules induced by Mg²⁺ or Ca²⁺,” *Biochem. Biophys. Res. Commun.* **155**(3), 1464–1470 (1988).
- ¹⁰H. H. Moon *et al.*, “Mitotic centromere-associated kinesin (MCAK/KIF2C) regulates cell migration and invasion by modulating microtubule dynamics and focal adhesion turnover,” *Cancers* **13**(22), 5673 (2021).
- ¹¹J. Průša *et al.*, “Electro-opening of a microtubule lattice in silico,” *Comput. Struct. Biotechnol. J.* **19**, 1488–1496 (2021).
- ¹²W. Guo *et al.*, “Using a comprehensive approach to investigate the interaction between Kinesin-5/Eg5 and the microtubule,” *Comput. Struct. Biotechnol. J.* **20**, 4305–4314 (2022).
- ¹³E. Nogales *et al.*, “Erratum: Structure of the $\alpha\beta$ tubulin dimer by electron crystallography,” *Nature* **391**, 199–203 (1998).
- ¹⁴L. J. Gagliardi and D. H. Shain, “Electrostatic forces drive poleward chromosome motions at kinetochores,” *Cell Div.* **11**, 14 (2016).
- ¹⁵J. A. Tuszyński *et al.*, “Molecular dynamics simulations of tubulin structure and calculations of electrostatic properties of microtubules,” *Math. Comput. Modell.* **41**(10), 1055–1070 (2005).
- ¹⁶A. Mershin *et al.*, “Tubulin dipole moment, dielectric constant and quantum behavior: Computer simulations, experimental results and suggestions,” *Biosystems* **77**(1-3), 73–85 (2004).
- ¹⁷S. Li, C. Wang, and P. Nithiarasu, “Electromechanical vibration of microtubules and its application in biosensors,” *J. R. Soc. Interface* **16**(151), 20180826 (2019).
- ¹⁸W. A. Nganfo *et al.*, “Dynamic behaviour of microtubules around the critical temperature and effect of the electric field produced by these vibrations on its environment,” *Eur. Phys. J. Plus* **136**(10), 1003 (2021).
- ¹⁹M. Cannariato *et al.*, “Mechanical communication within the microtubule through network-based analysis of tubulin dynamics,” *Biomech. Model. Mechanobiol.* **4**, 569–579 (2024).
- ²⁰P. Marracino *et al.*, “Tubulin response to intense nanosecond-scale electric field in molecular dynamics simulation,” *Sci. Rep.* **9**(1), 10477 (2019).
- ²¹J. Průša and C. Michal, “Electro-detachment of kinesin motor domain from microtubule in silico,” *Comput. Struct. Biotechnol. J.* **21**, 1349–1361 (2023).
- ²²N. B. Gudimchuk *et al.*, “Mechanisms of microtubule dynamics and force generation examined with computational modeling and electron cryotomography,” *Nat. Commun.* **11**(1), 3765 (2020).
- ²³X. Li, F. Yang, and B. Rubinsky, “A theoretical study on the biophysical mechanisms by which tumor treating fields affect tumor cells during mitosis,” *IEEE Trans. Biomed. Eng.* **67**(6), 2594–2602 (2020).
- ²⁴J. Tuszyński *et al.*, “An overview of sub-cellular mechanisms involved in the action of TTFields,” *Int. J. Environ. Res. Public Health* **13**(11), 1128 (2016).
- ²⁵Y. Zhao and G. Zhang, “Elucidating the mechanism of 200 kHz tumor treating fields with a modified DEP theory,” in *IEEE International Symposium on Signal Processing and Information Technology (ISSPIT)*, 2018.
- ²⁶E. Neuhaus *et al.*, “Alternating electric fields (TTFields) activate Ca_v1.2 channels in human glioblastoma cells,” *Cancers* **11**(1), 110 (2019).
- ²⁷B. Koltun *et al.*, “Tumor treating fields (TTFields) increase cancer cell membrane permeability and improve sensitivity to doxorubicin in vitro and in vivo,” *Cancer Res.* **84**(6), 4672 (2024).
- ²⁸K. Kwapiszewska *et al.*, “Nanoscale viscosity of cytoplasm is conserved in human cell lines,” *J. Phys. Chem. Lett.* **11**(16), 6914–6920 (2020).
- ²⁹T. Kalwarczyk *et al.*, “Comparative analysis of viscosity of complex liquids and cytoplasm of mammalian cells at the nanoscale,” *Nano. Lett.* **11**(5), 2157–2163 (2011).
- ³⁰M. G. L. van den Heuvel *et al.*, “Electrophoresis of individual microtubules in microchannels,” *Proc. Natl. Acad. Sci. U. S. A.* **104**(19), 7770–7775 (2007).
- ³¹W. F. Heinz and J. H. Hoh, “Relative surface charge density mapping with the atomic force microscope,” *Biophys. J.* **76**(1), 528–538 (1999).
- ³²R. P. Joshi, Q. Hu, and K. H. Schoenbach, “Modeling studies of cell response to ultrashort, high-intensity electric fields—implications for intracellular manipulation,” *IEEE Trans. Plasma Sci.* **32**(4), 1677–1686 (2004).
- ³³S. P. Alexander and C. L. Rieder, “Chromosome motion during attachment to the vertebrate spindle: Initial saltatory-like behavior of chromosomes and quantitative analysis of force production by nascent kinetochore fibers,” *J. Cell Biol.* **113**(4), 805–815 (1991).
- ³⁴P. Xie, “Molecular mechanism of processive stepping of kinesin motors,” *Symmetry* **13**(10), 1799 (2021).
- ³⁵P. Xie, “A model of processive walking and slipping of kinesin-8 molecular motors,” *Sci. Rep.* **11**(1), 8081 (2021).
- ³⁶X. Zhang *et al.*, “Dynamic topology of double-stranded telomeric DNA studied by single-molecule manipulation *in vitro*,” *Nucl. Acids Res.* **48**(12), 6458–6470 (2020).
- ³⁷I. Minoura and E. Muto, “Dielectric measurement of individual microtubules using the electroorientation method,” *Biophys. J.* **90**(10), 3739–3748 (2006).
- ³⁸J. Průša and C. Michal, “Molecular dynamics simulation of the nanosecond pulsed electric field effect on kinesin nanomotor,” *Sci. Rep.* **9**(1), 19721 (2019).
- ³⁹M. Annamalai, “Localization of energy in tubulin system using numerical analysis,” *Eur. Phys. J. Plus* **137**(6), 756 (2022).

⁴⁰C. E. Walczak, S. Cai, and A. Khodjakov, "Mechanisms of chromosome behaviour during mitosis," *Nat. Rev. Mol. Cell Biol.* **11**(2), 91–102 (2010).

⁴¹C. Sacristan *et al.*, "Dynamic kinetochore size regulation promotes microtubule capture and chromosome biorientation in mitosis," *Nat. Cell. Biol.* **20**(7), 800–810 (2018).

⁴²T. Xiao and X. Song, "A systematic way to extend the Debye–Huckel theory beyond dilute electrolyte solutions," *J. Phys. Chem. A* **125**(10), 2173–2183 (2021).

⁴³W. Guo *et al.*, "A comprehensive study on the electrostatic properties of tubulin-tubulin complexes in microtubules," *Cells* **12**(2), 238 (2023).